

## Supporting Information

### Ternary Organic Solar Cells: Compatibility Controls for Morphology Evolution of Active Layers

Qingyun Ai<sup>a</sup>, Weihua Zhou<sup>a,b</sup>, Lin Zhang<sup>c</sup>, Liqiang Huang<sup>b</sup>, Jingping Yin<sup>b</sup>,  
Zoukangning Yu<sup>a</sup>, Siqi Liu<sup>b</sup>, Wei Ma<sup>\*c</sup>, Jianrong Zeng<sup>\*d</sup>, Yiwang Chen<sup>\*a,b</sup>

<sup>a</sup>School of Materials Science and Engineering, Nanchang University, 999 Xuefu Avenue, Nanchang 330031, China

<sup>b</sup>College of Chemistry, Nanchang University, 999 Xuefu Avenue, Nanchang 330031, China

<sup>c</sup>State Key Laboratory for Mechanical Behavior of Materials, Xi'an Jiaotong University, 28 Xianning West Road, Xi'an 710049, China

<sup>d</sup>Shanghai Synchrotron Radiation Facility (SSRF), Shanghai Institute of Applied Physics, Chinese Academy of Sciences, 2019 Jialuo Road, Shanghai 201800, China

\*Corresponding author. Tel.: +86 791 83968703; fax: +86 791 83969561. E-mail:  
[ywchen@ncu.edu.cn](mailto:ywchen@ncu.edu.cn) (Y. Chen); [msewma@mail.xjtu.edu.cn](mailto:msewma@mail.xjtu.edu.cn) (W. Ma);  
[zengjianrong@sinap.ac.cn](mailto:zengjianrong@sinap.ac.cn) (J. Zeng).

Author contributions. Q. Ai and W. Zhou contributed equally to this work.

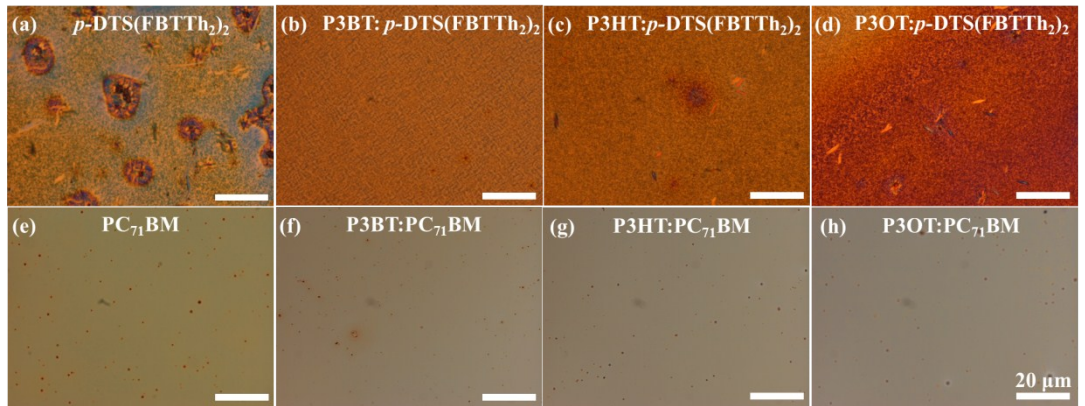


**Figure S1.** POM images of (a) *p*-DTS(FBTTh<sub>2</sub>)<sub>2</sub>, (b) P3BT:*p*-DTS(FBTTh<sub>2</sub>)<sub>2</sub>, (c) P3HT:*p*-DTS(FBTTh<sub>2</sub>)<sub>2</sub>, (d) P3OT:*p*-DTS(FBTTh<sub>2</sub>)<sub>2</sub>, (e) PC<sub>71</sub>BM, (f) P3BT:PC<sub>71</sub>BM, (g) P3HT:PC<sub>71</sub>BM, and (h) P3OT:PC<sub>71</sub>BM, respectively. The scale bar is 20  $\mu\text{m}$ .

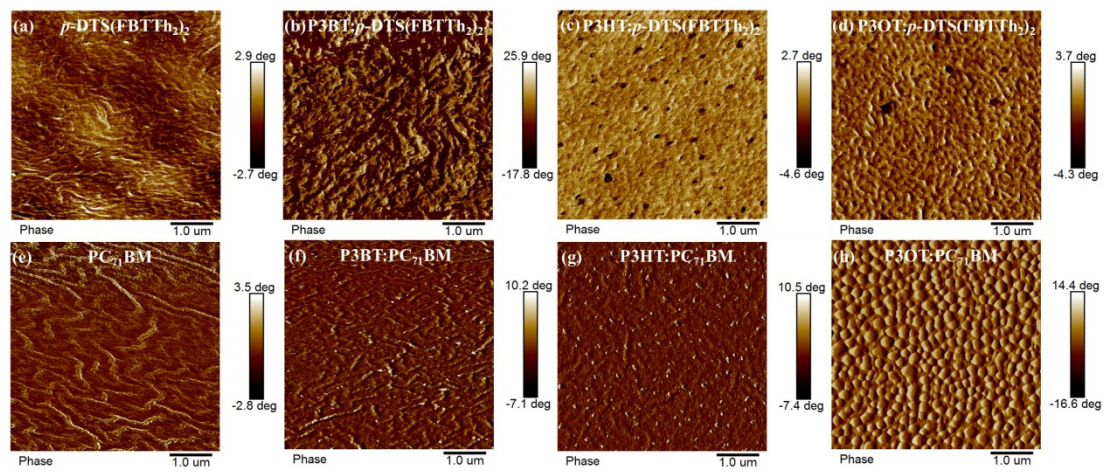


**Figure S2.** AFM phase images ( $5 \times 5 \mu\text{m}^2$ ) of (a) *p*-DTS(FBTTh<sub>2</sub>)<sub>2</sub>, (b) P3BT:*p*-DTS(FBTTh<sub>2</sub>)<sub>2</sub>, (c) P3HT:*p*-DTS(FBTTh<sub>2</sub>)<sub>2</sub>, (d) P3OT:*p*-DTS(FBTTh<sub>2</sub>)<sub>2</sub>, (e) PC<sub>71</sub>BM, (f) P3BT:PC<sub>71</sub>BM, (g) P3HT:PC<sub>71</sub>BM, and (h) P3OT:PC<sub>71</sub>BM, respectively.

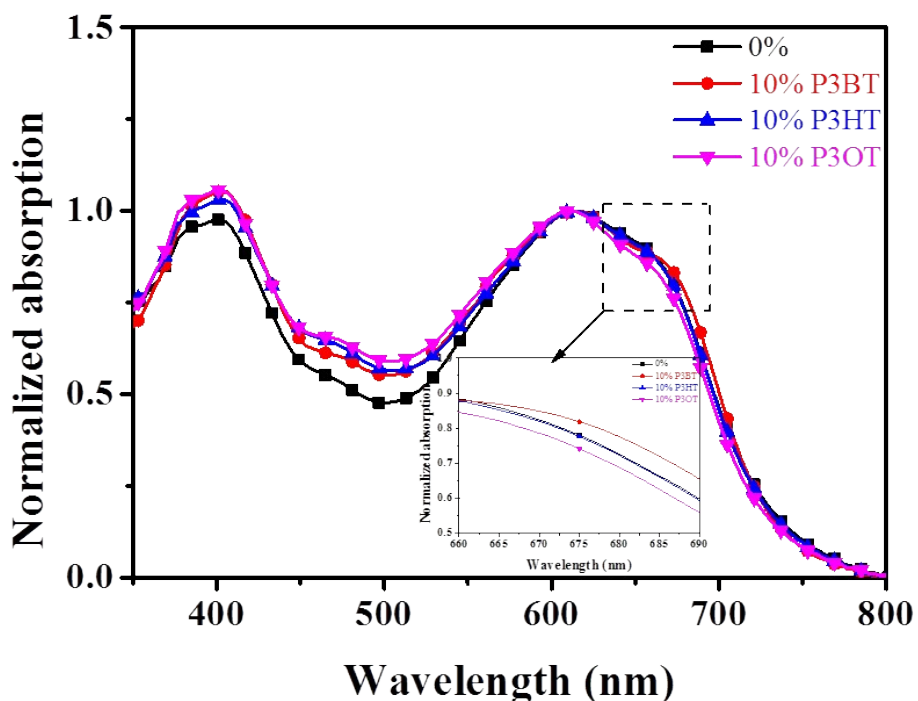


**Figure S3.** Normalized absorption spectra of the *p*-DTS(FBTTh<sub>2</sub>)<sub>2</sub>:PC<sub>71</sub>BM film containing 0 wt%, 10 wt% P3BT, 10 wt% P3HT, and 10 wt% P3OT, respectively.

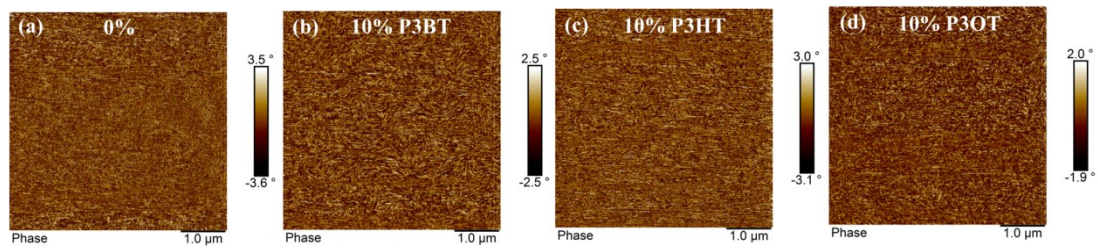


**Figure S4.** AFM phase images ( $5 \times 5 \mu\text{m}$ ) of *p*-DTS(FBTTh<sub>2</sub>)<sub>2</sub>:PC<sub>71</sub>BM film containing (a) 0 wt%, (b) 10 wt% P3BT, (c) 10 wt% P3HT, and (d) 10 wt% P3OT, respectively.

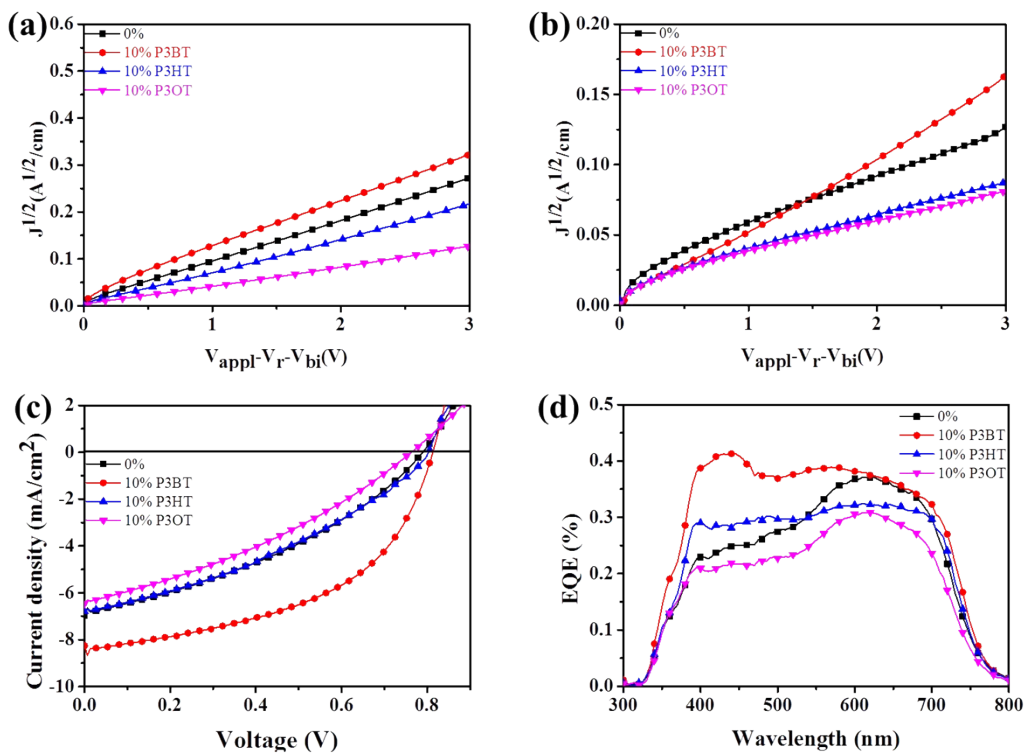


**Figure S5.**  $J^{1/2}$ - $V$  characteristics of (a) hole-only and (b) electron-only *p*-DTS(FBTTh<sub>2</sub>)<sub>2</sub>:PC<sub>71</sub>BM devices containing 0 wt%, 10 wt% P3BT, 10 wt% P3HT, and 10 wt% P3OT. (c)  $J$ - $V$  curve of *p*-DTS(FBTTh<sub>2</sub>)<sub>2</sub>:PC<sub>71</sub>BM solar cells containing 0 wt%, 10 wt% P3BT, 10 wt% P3HT, and 10 wt% P3OT. (d) The corresponding EQE measurements.

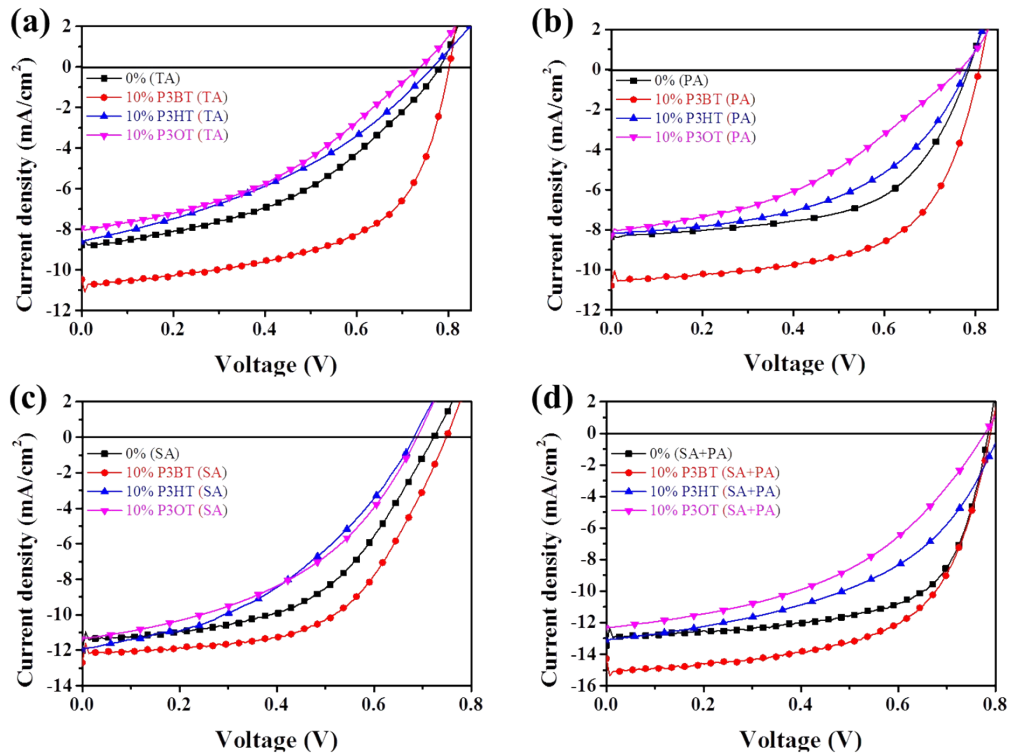


**Figure S6.** (a) *J-V* curves of *p*-DTS(FBTTh<sub>2</sub>)<sub>2</sub>:PC<sub>71</sub>BM solar cells containing 0 wt%, 10 wt% P3BT, 10 wt% P3HT and 10 wt% P3OT under four optimal conditions: (a) Thermal annealing at 70 °C for 10 min; (b) Post annealing at 100 °C for 10 min; (c) Solvent annealing 30 min; and (d) Solvent annealing 30 min and post-annealing at 100 °C for 10 min.

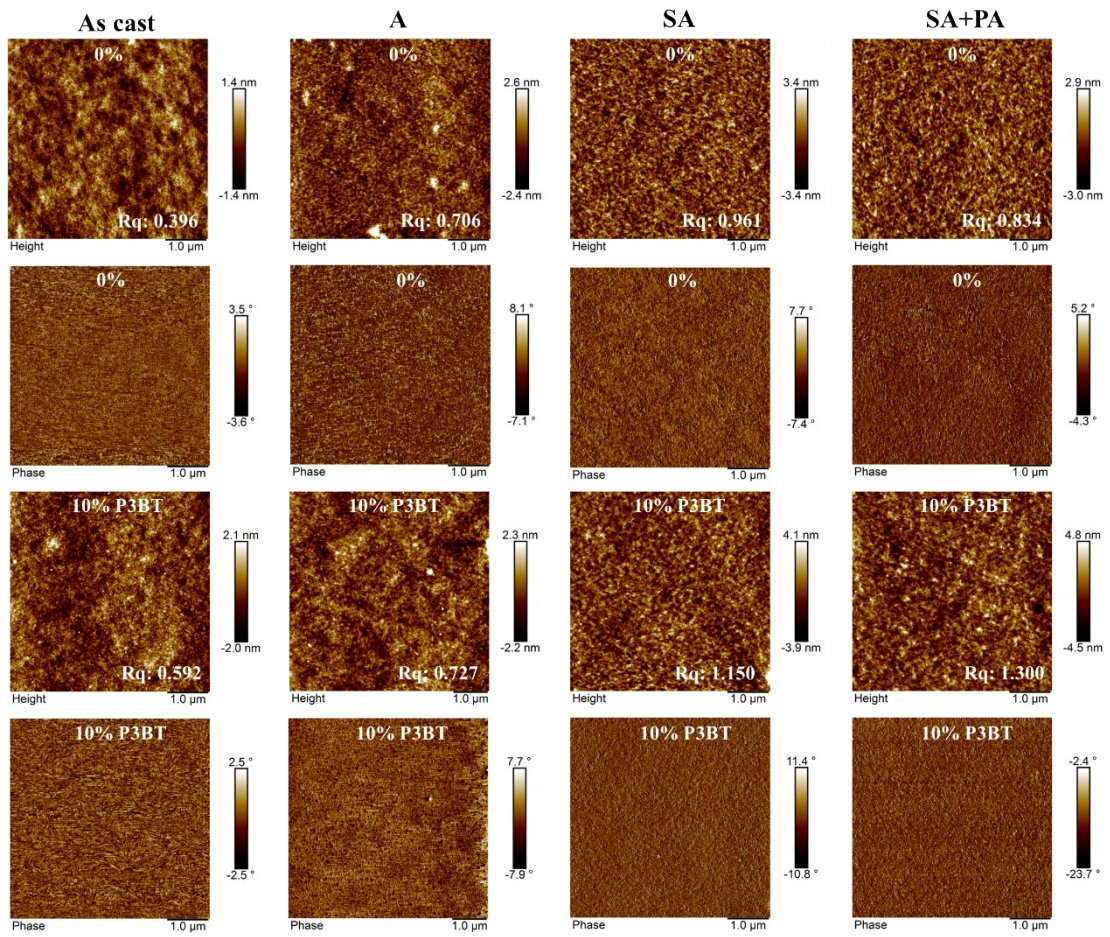


**Figure S7.** AFM height and phase images ( $5 \times 5 \mu\text{m}^2$ ) of *p*-DTS(FBTTh<sub>2</sub>)<sub>2</sub>:PC<sub>71</sub>BM film containing 0 wt%, 10 wt% P3BT under different annealing conditions.

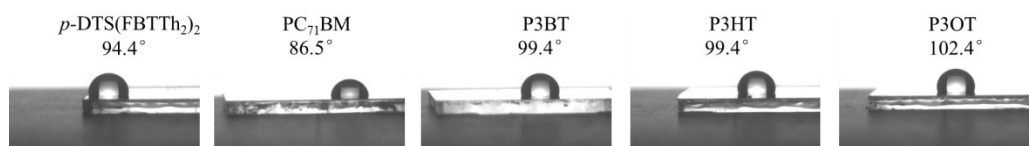


**Figure S8.** The contact angle measurements with water on the thin film of *p*-DTS(FBTTh<sub>2</sub>)<sub>2</sub>, PC<sub>71</sub>BM, P3BT, P3HT and P3OT.

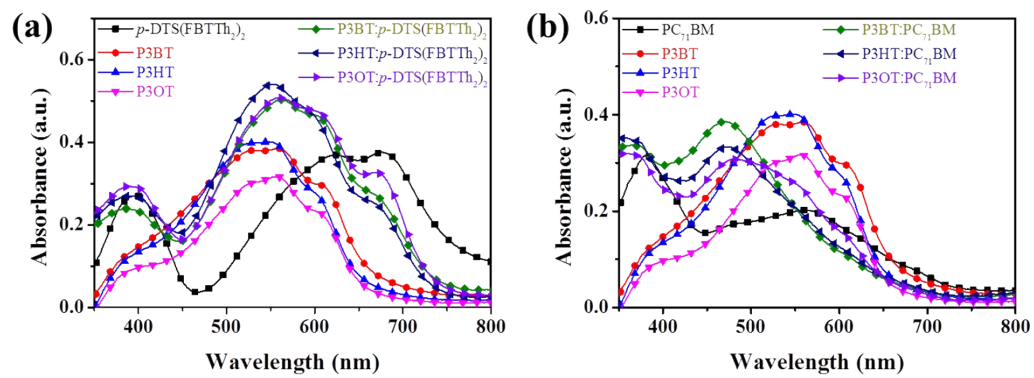


**Figure S9.** (a) UV-vis absorption spectra of *p*-DTS(FBTTh<sub>2</sub>)<sub>2</sub> and P3ATs:*p*-DTS(FBTTh<sub>2</sub>)<sub>2</sub> (1:1, w/w) blend. (b) UV-vis absorption spectra of PC<sub>71</sub>BM and P3ATs:PC<sub>71</sub>BM (1:1, w/w) blend.

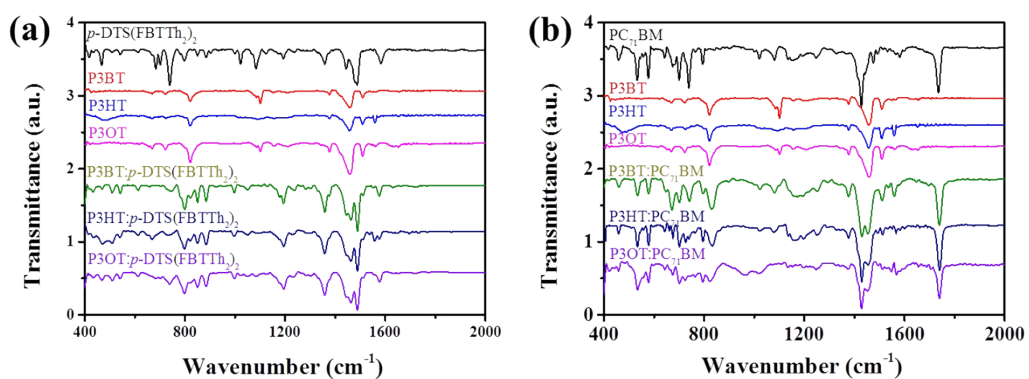


**Figure S10.** (a) FTIR spectra of *p*-DTS(FBTTh<sub>2</sub>)<sub>2</sub> and P3ATs:*p*-DTS(FBTTh<sub>2</sub>)<sub>2</sub> (1:1, w/w) blend. (b) FTIR spectra of PC<sub>71</sub>BM and P3ATs:PC<sub>71</sub>BM (1:1, w/w) blend.

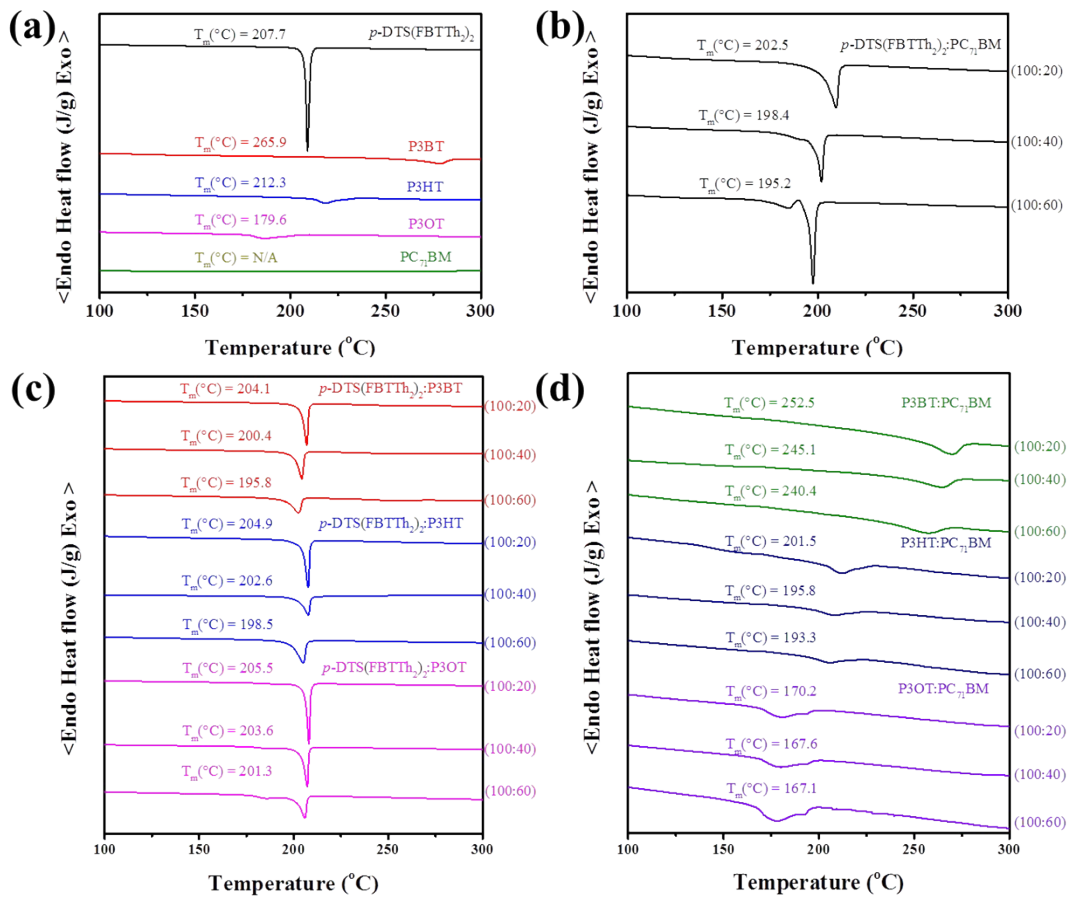


**Figure S11.** DSC heating curves of (a) *p*-DTS(FBTTh<sub>2</sub>)<sub>2</sub>, P3BT, P3HT, P3OT, and PC<sub>71</sub>BM; (b) *p*-DTS(FBTTh<sub>2</sub>)<sub>2</sub>:PC<sub>71</sub>BM blends; (c) *p*-DTS(FBTTh<sub>2</sub>)<sub>2</sub>:P3ATs blends; and (d) PC<sub>71</sub>BM:P3ATs blends with different weight ratio.

### The calculation of interaction parameters ( $\chi$ )

Measurement of the melting point temperature ( $T_m$ ) depression for blends was used to determine the Flory-Huggins interaction parameter ( $\chi$ ) of organic materials in the melting state. The larger the melting point depression, the smaller the value of  $\chi$ , and the greater the intermolecular interaction.<sup>2</sup> Equation 3 reflects the melting point depression of organic materials in the presence of a miscible diluent, as derived by Nishi and Wang:<sup>3</sup>

$$\frac{1}{T_m} - \frac{1}{T_m^0} = -\frac{R}{\Delta H_f} \frac{\nu_2}{\nu_1} \left[ \frac{\ln \Phi_2}{m_2} + \left( \frac{1}{m_2} - \frac{1}{m_1} \right) \times (1 - \Phi_2) + \chi (1 - \Phi_2)^2 \right] \quad (3)$$

where, the subscript 1 identified with the weaker crystalline material and 2 with the stronger crystalline material, respectively;  $T_m$  and  $T_m^0$  are the melting points of the mixture and the pure stronger crystalline material; R is the ideal gas constant,  $\Delta H_f$  is the heat of fusion of stronger crystalline material;  $v$  is the molar volumes,  $m$  is the degree of polymerization; and  $\Phi$  is the volume fraction.

For  $p$ -DTS(FBTTh<sub>2</sub>)<sub>2</sub>:PC<sub>71</sub>BM blends, the subscript 1 identified with the amorphous small molecule PC<sub>71</sub>BM and 2 with the crystalline small molecule  $p$ -DTS(FBTTh<sub>2</sub>)<sub>2</sub>, both  $m_1$  and  $m_2$  are 1; eq 3 therefore reduces to

$$\frac{1}{T_m} - \frac{1}{T_m^0} = -\frac{R}{\Delta H_f v_1} [\ln \Phi_2 + \chi(1 - \Phi_2)^2] \quad (4)$$

For P3ATs: $p$ -DTS(FBTTh<sub>2</sub>)<sub>2</sub> blends, the subscript 1 identified with the semicrystalline polymer P3ATs and 2 with the crystalline small molecule  $p$ -DTS(FBTTh<sub>2</sub>)<sub>2</sub>,  $m_1$  is very large compared to 1 and  $m_2$  is 1; eq 3 therefore reduces to

$$\frac{1}{T_m} - \frac{1}{T_m^0} = -\frac{R}{\Delta H_f v_1} [\ln \Phi_2 + (1 - \Phi_2) + \chi(1 - \Phi_2)^2] \quad (5)$$

For P3ATs:PC<sub>71</sub>BM blends, the subscript 1 identified with the amorphous PC<sub>71</sub>BM and 2 with the semicrystalline polymer P3ATs,  $m_1$  is 1 and  $m_2$  is very large compared to 1; eq 3 therefore reduces to

$$\frac{1}{T_m} - \frac{1}{T_m^0} = -\frac{R}{\Delta H_f v_1} [-(1 - \Phi_2) + \chi(1 - \Phi_2)^2] \quad (6)$$

By neglecting the effect of entropy and  $\Phi_2$ ,  $\chi$  can have the following form

$$\chi = \frac{Bv_1}{RT} \quad (7)$$

where B is the interaction energy density characteristic of the organic material pair.

Substituting eq 7 into eq 4, eq 5, and eq 6 yields

$$\frac{1}{\Phi_1} \left( \frac{1}{T_m} - \frac{1}{T_m^0} + \frac{R}{\Delta H_f v_1} \times \ln \Phi_2 \right) = -\frac{Bv_2 \Phi_1}{\Delta H_f T_m} \quad (8)$$

$$-\frac{1}{\Phi_1} \left[ \frac{1}{T_m} - \frac{1}{T_m^0} + \frac{R \ v_2}{\Delta H_f v_1} \times (\Phi_1 + \ln \Phi_2) \right] = \frac{R \ v_2}{\Delta H_f v_1} + \frac{B v_2 \Phi_1}{\Delta H_f T_m} \quad (9)$$

$$\frac{1}{\Phi_1} \left( \frac{1}{T_m} - \frac{1}{T_m^0} \right) = \frac{R \ v_2}{\Delta H_f v_1} - \frac{B v_2 \Phi_1}{\Delta H_f T_m} \quad (10)$$

From eq 8, eq 9, and eq 10 yields three linear relationship between  $(1/T_m - 1/T_m^0 + Rv_2 \ln \Phi_2 / \Delta H_f v_1) / \Phi_1$  and  $\Phi_1 / T_m$ ,  $-(1/T_m - 1/T_m^0 + Rv_2(\Phi_1 + \ln \Phi_2) / \Delta H_f v_1) / \Phi_1$  and  $\Phi_1 / T_m$ ,  $(1/T_m - 1/T_m^0) / \Phi_1$  and  $\Phi_1 / T_m$ ; respectively.  $\chi$  can be extracted by the slope  $b$  of the linear fit straight line. Due to the temperature of the active layer heating and spin coating is 90 °C, so the final calculated  $\chi$  value is the interaction parameter of blends at 90 °C.

**Table S1.** Summary of the hole and electron mobility,  $\mu_h$  and  $\mu_e$  and their ratio  $R_\mu$  ( $= \mu_e/\mu_h$ ) of *p*-DTS(FBTTh<sub>2</sub>)<sub>2</sub>:PC<sub>71</sub>BM device containing 0 wt%, 10 wt% P3BT, 10 wt% P3HT, and 10 wt% P3OT.

Additive content (wt %)	$\mu_h$ (cm <sup>2</sup> /V·s)	$\mu_e$ (cm <sup>2</sup> /V·s)	$\mu_h/\mu_e$
0%	$2.24 \times 10^{-4}$	$3.40 \times 10^{-5}$	6.59
10% P3BT	$2.83 \times 10^{-4}$	$8.89 \times 10^{-5}$	3.18
10% P3HT	$1.68 \times 10^{-4}$	$1.72 \times 10^{-5}$	9.77
10% P3OT	$5.58 \times 10^{-5}$	$1.45 \times 10^{-5}$	3.85

**Table S2.** Summary of the photovoltaic parameters of *p*-DTS(FBTTh<sub>2</sub>)<sub>2</sub>:PC<sub>71</sub>BM solar cells containing different weight ratios of P3BT, P3HT, and P3OT under AM 1.5G solar illumination.

Additive content (wt)	$J_{sc}$ (mA/cm <sup>2</sup> )	$V_{oc}$ (V)	FF (%)	PCE (%)
0%	6.97	0.786	35.7	2.0
5% P3BT	7.66	0.806	44.2	2.7
10% P3BT	8.25	0.812	50.9	3.4
20% P3BT	5.86	0.811	39.2	1.9
5% P3HT	6.87	0.796	37.8	2.1
10% P3HT	6.80	0.797	35.4	1.9
20% P3HT	5.92	0.794	36.5	1.7
5% P3OT	5.85	0.798	36.9	1.7
10% P3OT	5.67	0.765	31.5	1.4
20% P3OT	4.97	0.737	36.4	1.3

**Table S3.** Surface energy, wetting coefficients, and predicted location of P3BT, P3HT and P3OT within the *p*-DTS(FBTTh<sub>2</sub>)<sub>2</sub>:PC<sub>71</sub>BM matrices.

Materials	Surface energy (mN m <sup>-1</sup> )	Wetting coefficient (ω <sub>C</sub> )	Predicated location of P3ATs in the blends
<i>p</i> -DTS(FBTTh <sub>2</sub> ) <sub>2</sub>	26.46		
PC <sub>71</sub> BM	31.39		
P3BT	23.43	2.24	in <i>p</i> -DTS(FBTTh <sub>2</sub> ) <sub>2</sub>
P3HT	23.43	2.24	in <i>p</i> -DTS(FBTTh <sub>2</sub> ) <sub>2</sub>
P3OT	21.56	3.02	in <i>p</i> -DTS(FBTTh <sub>2</sub> ) <sub>2</sub>

### The calculation of wetting coefficient (ω<sub>C</sub>)

The wetting coefficient of material C (ω<sub>C</sub>) in blends of materials A and B can be calculated by Young's equation as follows:<sup>1</sup>

$$\omega_C = \frac{\gamma_{C-B} - \gamma_{C-A}}{\gamma_{A-B}} \quad (1)$$

where γ<sub>X-Y</sub> is the interfacial surface energy between X and Y. The interfacial surface energy can be calculated by Neumann's equation as follows:

$$\begin{aligned} \gamma_{X-Y} \\ = \gamma_X + \gamma_Y - 2(\gamma_X \times \gamma_Y)^{0.5} e^{[-\beta(\gamma_X + \gamma_Y)^2]} \end{aligned}$$

where β = 0.000115 m<sup>4</sup> mJ<sup>-2</sup>. If ω<sub>C</sub> > 1, the material C will be located in the domain A; If ω<sub>C</sub> < -1, C will be located in the domain B; If -1 < ω<sub>C</sub> < 1, C will be located in the interface between A and B.

**Table S4.** The related parameters of *p*-DTS(FBTT<sub>2</sub>)<sub>2</sub>, PC<sub>71</sub>BM, P3BT, P3HT, and P3OT for calculated Flory-Huggins interaction parameter.

Materials	Melting point (°C)	Enthalpy (J/g)	Density (g/cm <sup>3</sup> )	Molar volume (cm <sup>3</sup> /mol)
<i>p</i> -DTS(FBTT <sub>2</sub> ) <sub>2</sub>	207.7	69.05	1.15	1059
PC <sub>71</sub> BM	/	/	1.3	793
P3BT	265.9	27.95	1.1	125
P3HT	212.3	23.35	1.1	151
P3OT	179.6	21.74	1.1	176

## REFERENCES

1. Honda, S.; Ohkita, H.; Benten, H.; Ito, S., Selective dye loading at the heterojunction in polymer/fullerene solar cells. *Adv. Energy Mater.* **2011**, 1, 588-598.
2. Ghasemi, M.; Ye, L.; Zhang, Q.; Yan, L.; Kim, J. H.; Awartani, O.; You, W.; Gadisa, A.; Ade, H., Panchromatic Sequentially Cast Ternary Polymer Solar Cells. *Adv. Mater.* **2017**, 29, 1604603.
3. Nishi, T.; Wang, T., Melting point depression and kinetic effects of cooling on crystallization in poly (vinylidene fluoride)-poly (methyl methacrylate) mixtures. *Macromolecules* **1975**, 8, 909-915.